

First Guess at Appropriate Time (FGAT) with WRF 3DVAR

Mi-Seon Lee, Dale Barker, Wei Huang, and Ying-Hwa Kuo

National Center for Atmospheric Research, P. O. Box 3000, Boulder, CO, 80307

1. Introduction

In OI or 3DVAR systems, observations collected within an observation window (normally ± 1 or ± 3 hr around the analysis time) are assumed to be valid at the analysis time and only one background (a short-range forecast valid at the analysis time) is used. This can potentially lead to inaccurate innovation vectors (observation minus background differences) for fast moving weather systems and for observations with wide time distribution, such as a single path of a polar-orbiting satellite. Like 4DVAR, FGAT compares the observations with the background at the observation time. However, instead of propagating the innovation by \mathbf{M} and \mathbf{M}^T in 4DVAR (notations by Courtier *et al.* 1994), FGAT assumes the innovation vector to be constant both in time and space within the observation window, as in the 3DVAR algorithm. The advantages of FGAT can be shown for cases when a low or high pressure system approaches a station. Main purpose of this study is to implement FGAT into the WRF 3DVAR system and to assess its impacts.

2. Basic Descriptions of observation data, 3DVAR, and model

Basic description of WRF 3DVAR can be found in Barker *et al.* (2003; 2004). The WRF 3DVAR system follows WRF model's software architecture (Michalakes *et al.*, 2002) and IO structure. In this study, we use $\psi, \chi_u, P_s, q, T_u$ as the control variables, and spatially inhomogeneous covariance for background error statistics (Wu *et al.*, 2003) in 3DVAR.

WRF model version 1.3 is used for performance test by FGAT. This model is characterized by nonhydrostatic equations with mass coordinate (Skamarock, 2002). We use NCEP 3 class microphysics option, nonlocal boundary layer, new Kain-Fritsch scheme for convection, and RRTM (Rapid Radiative Transfer Model) for long wave radiation (Dudhia, 2002).

For statistical results, we use 10 day period from 1 to 10 January 2002. Observation data used in this study include: Sound, Synop, Metar, Buoy, Ship, AMDAR, Pilot, Airep, Profiler, SATOB, SATEM, and QSCAT. Observations obtained with fast moving platforms are likely to be sensitive to FGAT. In order to assess the impact of FGAT, we include SATOB, SATEM, and QSCAT over the ocean. Model horizontal grid resolution is very coarse at 100km. Horizontal mesh size is 90 X 90 with 28 levels in the vertical. Figure 1 show the model domain and the distribution of QSCAT data with 25km resolution. This data will be thinned according to model resolution.

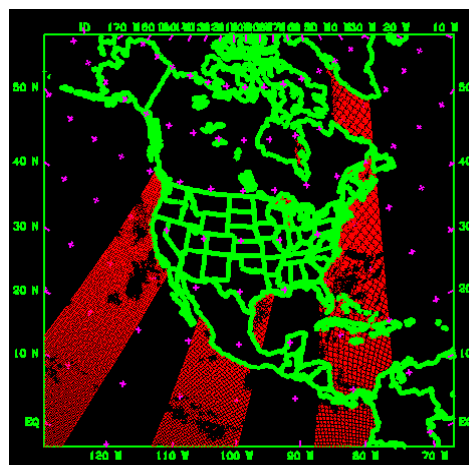


Fig. 1 Model domain and QSCAT data: 2001-Dec-31-21 UTC ~ 2002-Jan-1-03 UTC

3. FGAT implementation

We have chosen 6hr data assimilation cycle with ± 3 hr observation cutoff for this study. We assume that observations within 1hr time slot can use the same background. Followings are steps to perform the FGAT using WRF 3DVAR and model.

First, we divide the assimilation window (e.g., 00 UTC ± 3 hr) into 7 one-hour time slots (e.g., each time slot at 21, 22, 23, 00, 01, 02, 03 UTC).

Second, we sort observations y into each observation time slot, y_i ($y_i, i=1, 7$) using

Address for correspondence: National Center for Atmospheric Research, Boulder, CO, 80301.
E-mail: mslee@ucar.edu or mslee@kma.go.kr

observation pre-process (3DVAR_OBSPROC, Barker *et al.*, 2003). Each time slot has 1hr window (e.g., 20:30 ~ 21:29 for 21 UTC time slot).

Third, 3DVAR will read a first guess at the appropriate time for each time slot. These first-guess fields (e.g. -3, -2, -1, 0, +1, +2, +3) have been prepared by running the WRF model from the previous analysis.

Fourth, the 3DVAR system computes innovation vector for each time slot and add them together by the following equation.

$$y - H[M(x^b)] = \sum_{i=1}^7 y_i - H\{[M(x^b)]_i\}$$

Finally, after the innovation vector is obtained, the remaining step of minimization is exactly the same as the standard 3DVAR procedure.

Although the idea and mathematical formulation of FGAT is simple, practical implementation requires handling of multiple backgrounds and splitting observations in time are not straightforward under the WRF 3DVAR framework.

4. Results

a. Comparison of initial cost function

In order to have a clean comparison, we first examine the differences between the first cycle of R3DV (standard 3DVAR with single background analysis time) and that of FGAT (with 7 backgrounds from -3 to +3 h). First cycle mean that we start both experiments from the same initial model state, which is a 6-h forecast of WRF model based on AVN analysis. Figure 2 shows the initial cost function of standard 3DVAR (R3DVAR) and the difference of the two experiments over a 10 days period at 6 hour intervals. Positive difference indicates that FGAT has smaller initial cost function representing closer conformity of backgrounds to observations. In case of no SATEM and QSCAT data, major differences of initial cost function occur at 06 and 18 UTC not at 00 and 12 UTC. This is caused by our experimental data sets. Metar data from NCAR mass storage are equally distributed at 06 and 18 UTC for each time slot over the US domain. However we used only AVN data sets at 00 and 12 UTC which provide only one METAR data at one location over -3hr ~ +3hr window.

Without SATEM and QSCAT, difference of initial cost function between these two experiments is about 5% (e.g. 2,000 / 40,000 \approx 5%). However differences of initial cost function are increased when SATEM and QSCAT data are assimilated due to the characteristics of observation time of these

two types of observations. Roughly 10 % (5,000 / 50,000) of initial cost function was reduced by FGAT. Therefore we can see that departure of observations and background is reduced by use of multiple backgrounds in calculating innovation vector.

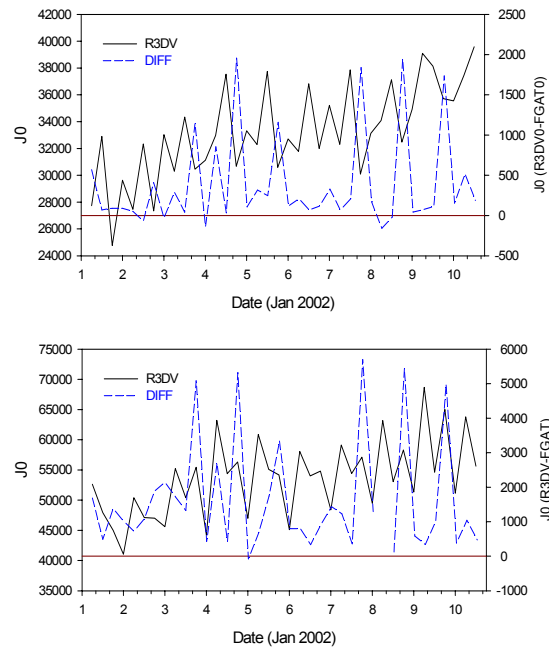


Fig. 2 Initial cost function (left axis) from standard 3DVAR (R3DV) and differences from R3DV-FGAT (right axis). Upper and lower panel indicate the results without and with the assimilation of SATEM and QSCAT data, respectively.

b. Observation data screening and IV and AO RMSE by different observation types

Current 3DVAR system includes a data screening procedure through CHECK_MAX_IV which is designed to filter the observation data with large departure of innovation vector (IV). Thus, if observations are closer to the background, we will have more observation data for the minimization procedure. Figure 3 shows the data number by this 3DVAR screening module according to observation type. Furthermore, RMSE of IV and departure of analysis and observations (A - O) are presented in Figure 3. Every value in figure was averaged over a 10 day period at 6 hour intervals. On average, 150

more surface data can be used with the use of FGAT method and 50 more for SATEM and QSCAT. Smaller IV and A - O are found with FGAT for SYNOP, AIREP, SHIP, SATEM, and QSCAT data. This means that observation data from moving platform are strongly affected by FGAT procedures. SYNOP (mainly METAR) data also are affected by FGAT procedure because of the frequent observation time during assimilation window.

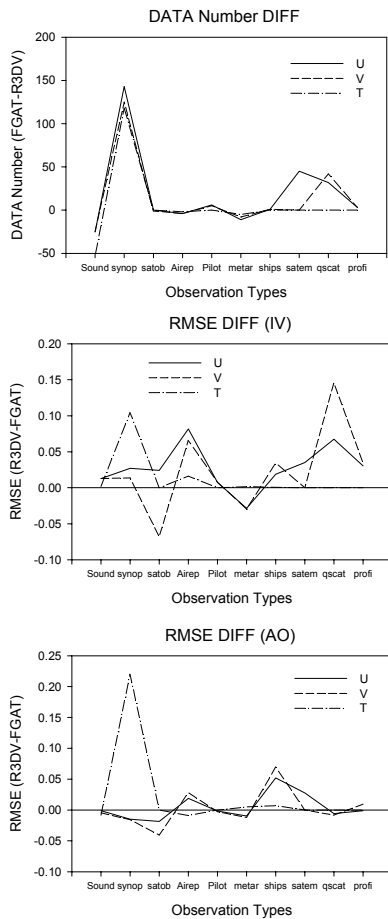


Fig. 3 Differences of data number used in 3DVAR (upper panel), IV RMSE (middle panel), and (c) A - O RMSE (lower panel) between R3DV and FGAT experiments in terms of observation types. All values are averaged over a 10-day period at 6 hour intervals.

c. Forecast impacts for a 100-km WRF model

We examine the forecast errors of standard 3DVAR (R3DV) and FGAT experiments. Major changes introduced by FGAT most likely occur over oceans due to aircraft and satellite observations. Nevertheless verification of forecasts against observation only over land indicates slight positive impacts of FGAT (Figure 4) for 2-day forecasts. RMS differences (R3DV-FGAT) for temperature become larger with the assimilation of SATEM and QSCAT data. The longer forecast time, the larger difference of RMSE between R3DV and FGAT is found in this study.

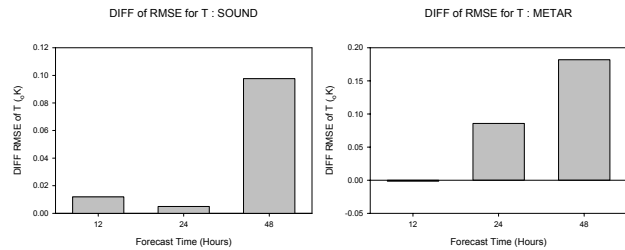


Fig. 4 Forecast error Differences (R3DV-FGAT) in terms of 10 day averaged RMSE against observation data. Left and right panel indicate temperature RMSE for experiments with SATEM and QSCAT against SOUND and METAR, respectively. Positive value means that R3DV has larger error than FGAT. 48-h forecasts are performed.

d. FGAT impacts on 6hr continuous cycling system

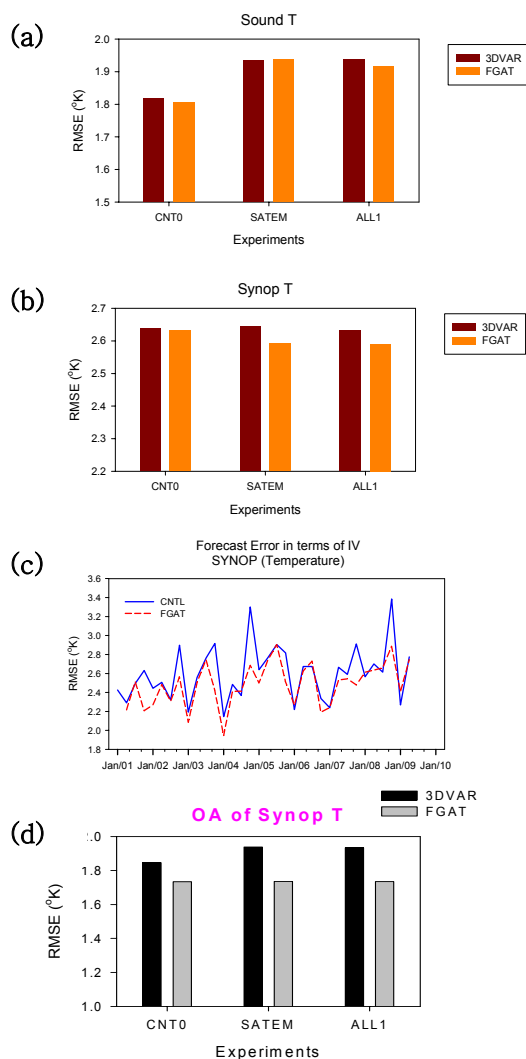
Because most operational centers use the continuous data assimilation system, we try to find the impact of FGAT on cycling 3DVAR system. Backgrounds are generated continuously by WRF model from previous analysis (6hr before). In Figure 5, CNT0, SATEM, and ALL1 designate experiments without SATEM and QSCAT, with only SATEM, and with SATEM and QSCAT, respectively. IV means 6hr forecast error against observations in the 6hr continuous cycling system. Generally 3DVAR experiments do not show improvements from the assimilation of SATEM thickness and QSCAT winds. Even though FGAT also shows the similar trend as R3DV with single backgrounds, FGAT has reduced RMS error especially for surface data. In A - O statistics, FGAT with the assimilation of SATEM and QSCAT do not degrade the analysis at least, however, standard 3DVAR shows the increased RMSE.

6. Conclusions

Performing FGAT with WRF 3DVAR over a 10-day period (almost 40 cases) indicate positive impacts in terms of initial cost function, IV, A - O, and forecast RMS errors. As we expected originally, major impacts of FGAT occurred in observations with fast moving platform such as PILOT, Aircraft, Satellite data, and ship.

This study shows the verification results against observation over land. However, because FGAT probably has the largest impact over ocean, we need to perform the verification against analysis.

Significant positive impacts by FGAT are likely for rapidly propagating weather systems and for observations taken by fast moving platforms. So we need to investigate the impacts of FGAT on specific weather events.



Acknowledgment

This research was supported by the Post-doctoral Fellowship Program (2002) of Korea Science & Engineering Foundation (KOSEF), MMM Division Visitor Program, and the Air Force Weather Agency.

References

- Barker, D. M., Huang, W., Guo, Y-R., and Bourgeois, A1, 2003: *A three-dimensional Variational (3DVAR) Data Assimilation System for use with MM5*. NCAR Technical Note, NCAR/TN-453+STR, pp68.
- Barker, D. M., Huang, W., Guo, Y-R., and Xiao, Q. N. 2004: A three-Dimensional Variational Data Assimilation System for MM5: Implementation and initial results. *Mon. Wea. Rev.*, Submitted
- Coutier, P., J.-N. Thepaut and A. Hollingworth, 1994: A strategy for operational implementation of 4D-VAR, using incremental approach. *Q. J. R. Meteorol. Soc.*, **120**, 1367-1387.
- Michalakes, J., W. Skamarock, J. Dodhia, and D. Gill, 2002: WRF software development and performance. Preprints. *The Third WRF Users' workshop*. NCAR, Boulder, Co.
- Wu W.-S, R. J. Purser, and D. F., Parrish, 2003: Three-dimensional variational analysis with spatially inhomogeneous covariances. *Mon. Wea. Rev.* **130**. 2905-2916.
- Skamarock, B, 2002: The mass coordinate WRF model. Preprint. *The Third WRF Users' workshop*. NCAR, Boulder, Co.
- Didhia, J. 2002: WRF physics update. . Preprint. *The Third WRF Users' workshop*. NCAR, Boulder, Co.

Fig. 5 FGAT impacts in terms of IV RMSE against (a) SOUND and (b) SYNOP temperature. Backgrounds are generated by 6 hour continuous cycling system. (c) is time series for ALL1 experiment of IV RMSE against SYNOP temperature. (d) indicates A - O (analysis - observation) statistics against SYNOP temperature.